Supporting Information

Flexible and Transparent Cellulose Based Ionic Film as Humidity Sensor

Yang Wang,[ab] *Lina Zhang,* [ab] *Jinping Zhou,* [ab] *and Ang Lu*[*ab]

[a] College of Chemistry and Molecular Sciences, Wuhan University, Wuhan 430072, China

[b] Hubei Engineering Center of Natural Polymer-based Medical Materials, Wuhan University, Wuhan 430072, China

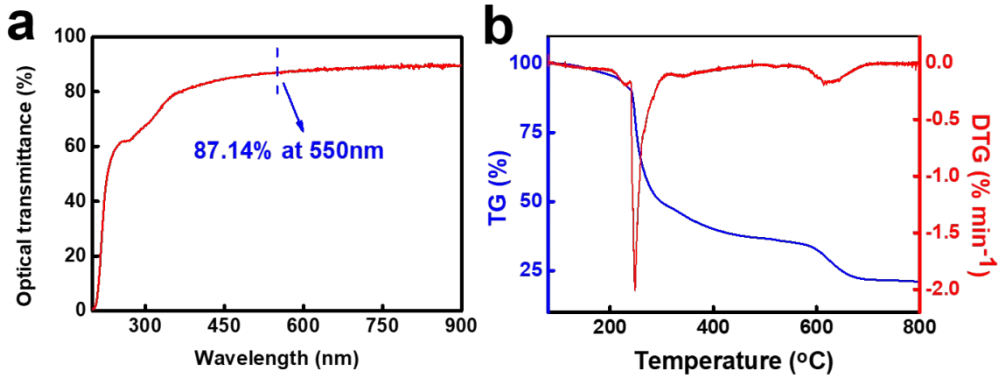

Figure S1. (a) Optical transmittance of CKF in the wavelength range from 210 to 900 nm. (b) Differential thermogravimetric and TGA thermograms of CKF in an air atmosphere.

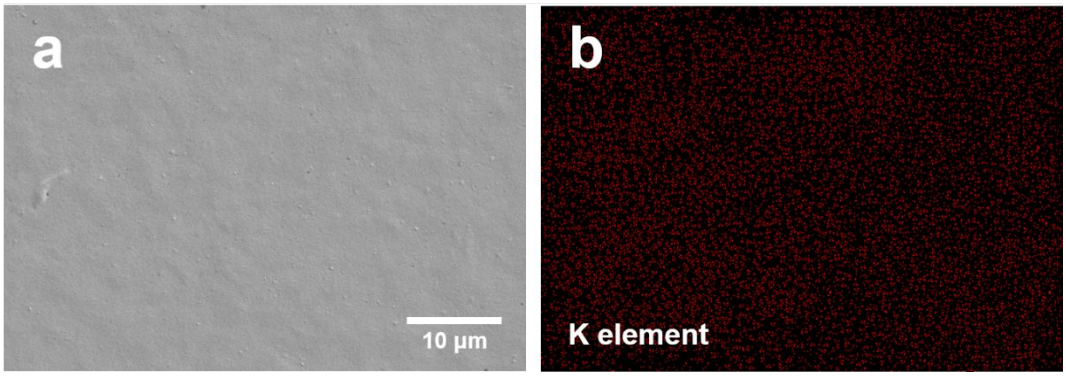

Figure S2. (a) Surface SEM images of CKF and (b) its distribution of potassium.

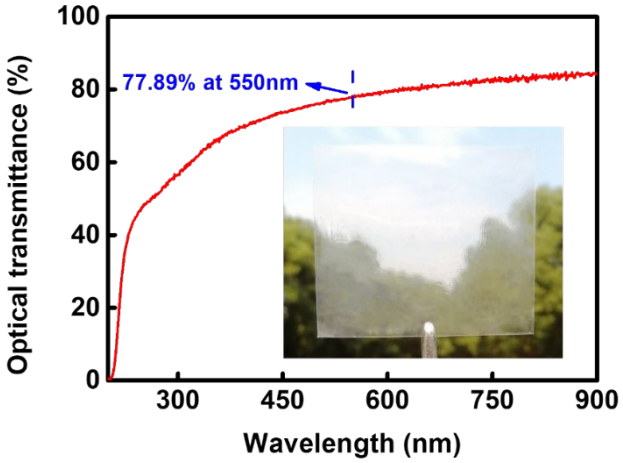

Figure S3. Optical transmittance of CKF-0 in the wavelength range from 210 to 900 nm, the inset is the photograph of CKF-0.

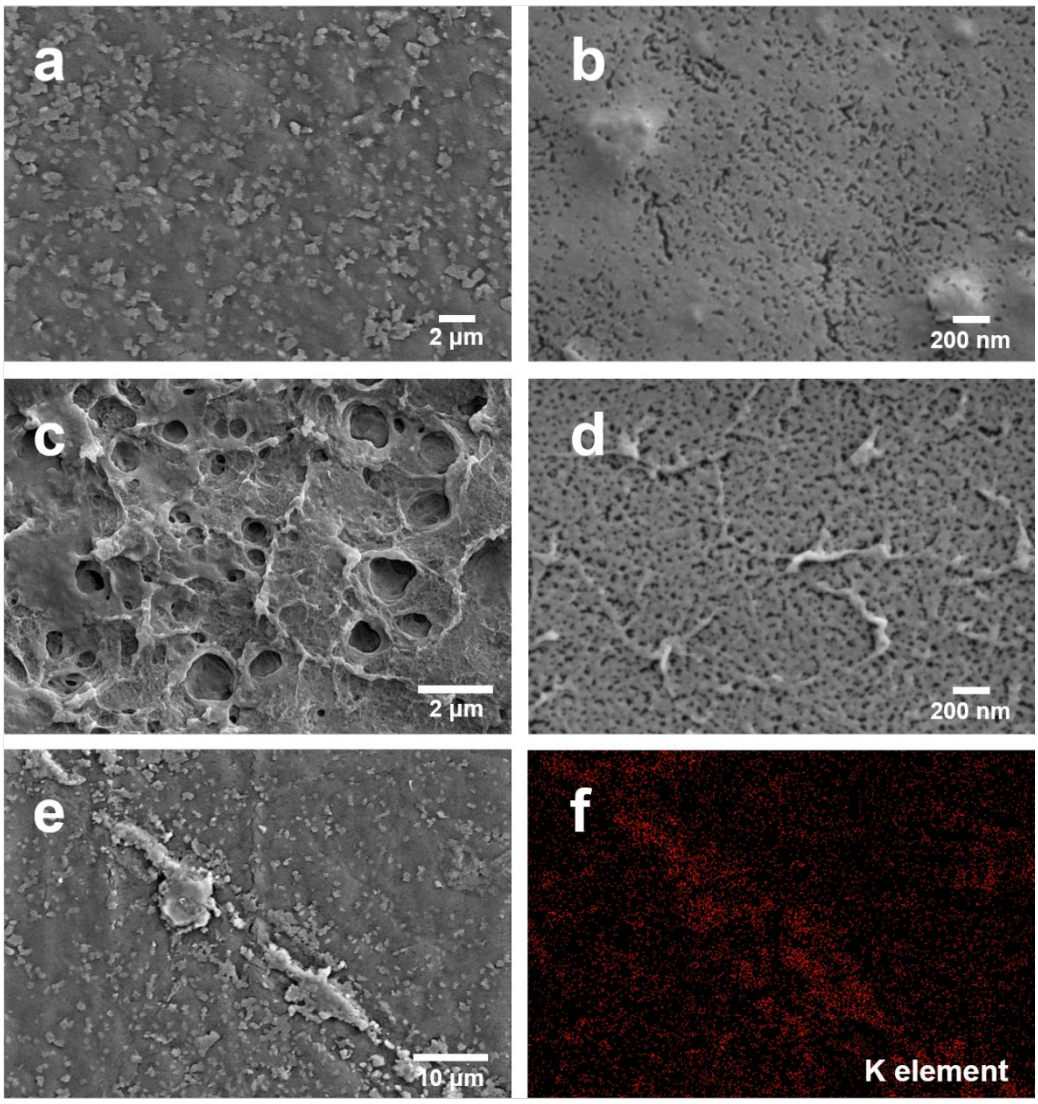

Figure S4. (a-b) Surface SEM image of CKF-0. (c-d) Surface SEM image of CF-0. (e) A gathering place of KOH on the surface of CKF-0 and (f) its distribution of potassium.

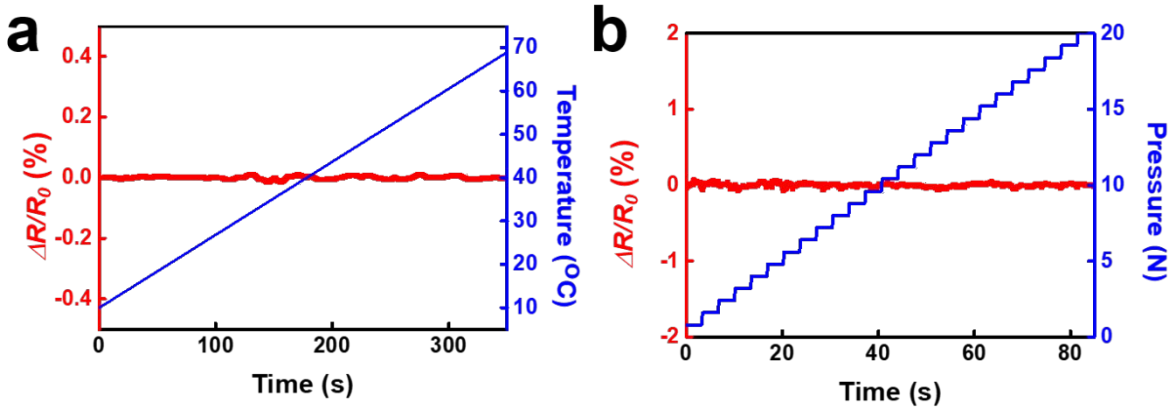

Figure S5. (a) Relative resistance variation ($\Delta R/R_0$) of CKF maintained as temperature changed from 10 to 70 °C. (b) $\Delta R/R_0$ of CKF maintained as pressure increased step-wise from 0 to 20 N (applied force area of 1.67 cm^{-2}).

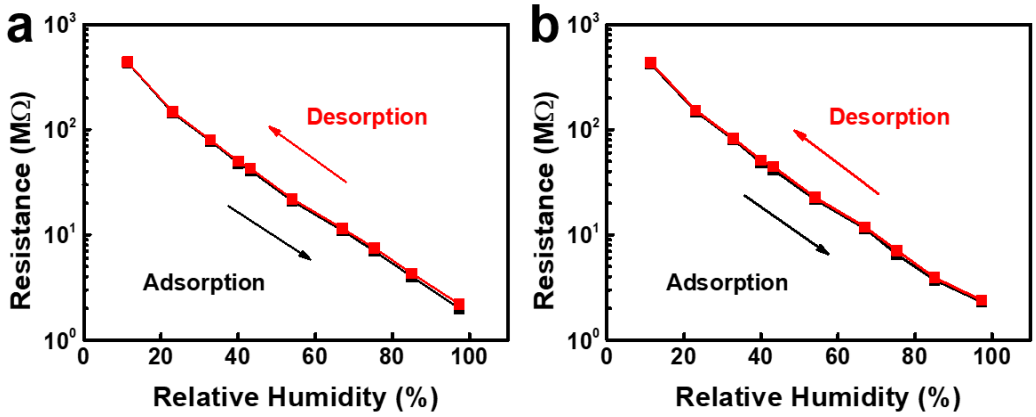

Figure S6. Adsorption/desorption curves of CKF before (a) and after (b) 1000 bending cycles.

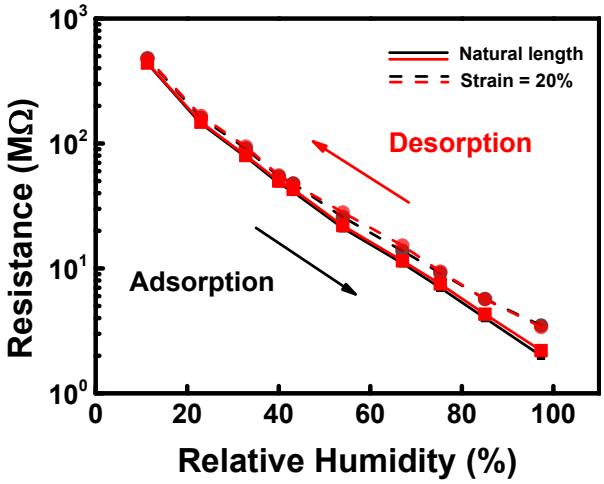

Figure S7. Adsorption/desorption curves with and without 20 % tensile strain.

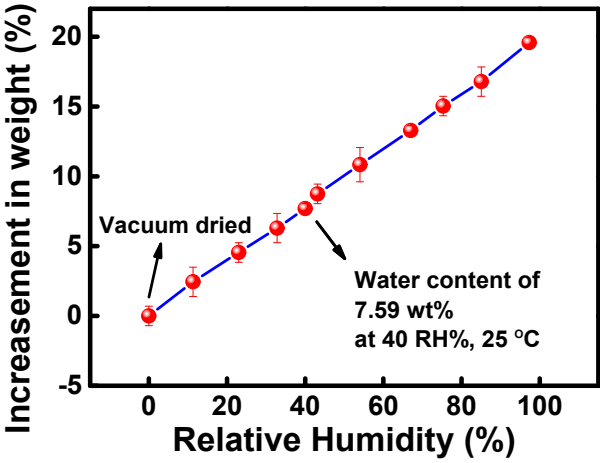

Figure S8. Weight change of CKF in air with different RH at room temperature.

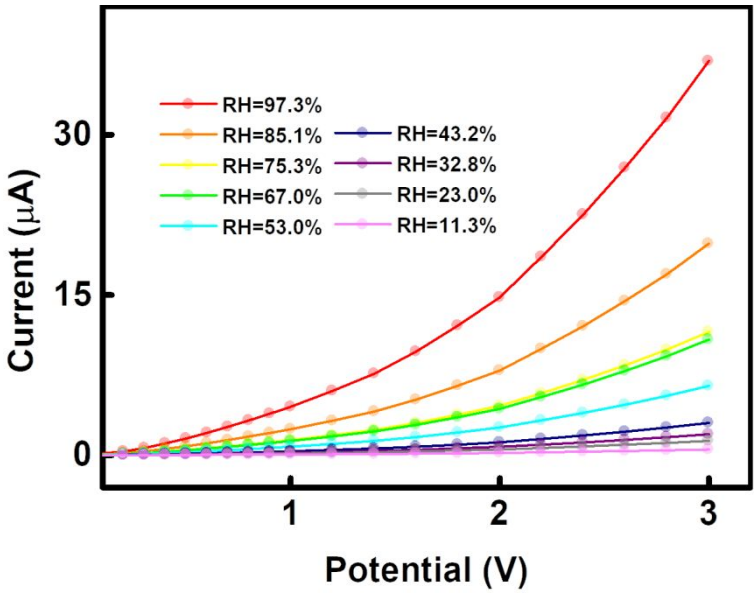

Figure S9. Current–voltage (I–V) characteristics of CKF under different RHs, within the voltage of 3V.

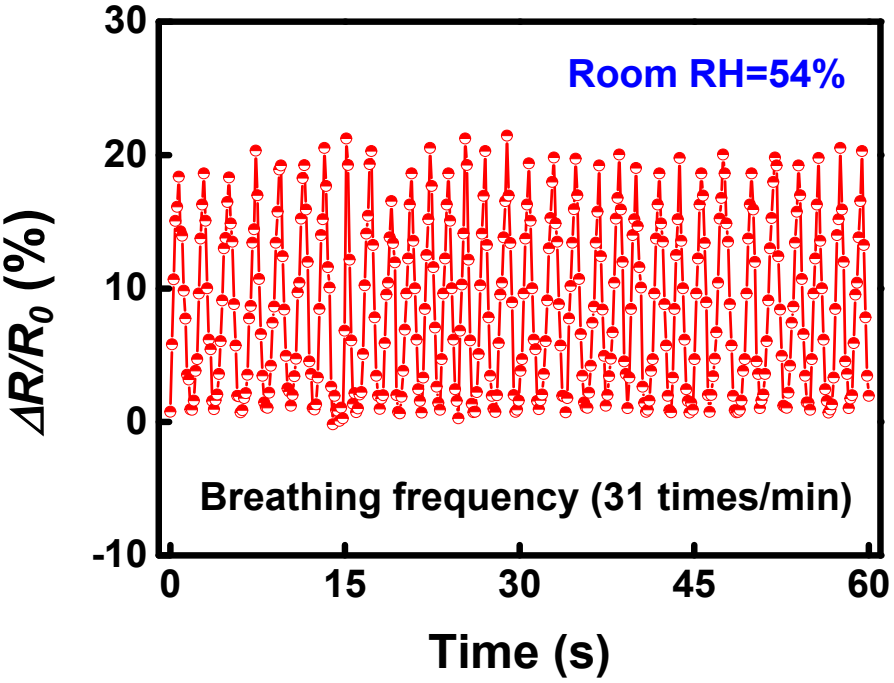

Figure S10. The detection of adult breathing after strenuous exercise.

Table S1. Comparison of the response and recovery times, and hysteresis of the humidity sensor devices based on various nanomaterials.

Sensing materials	Response time [s]	Recover time [s]	Hysteresis [%]	Device	Transparent	Ref.
Silicon-nanocrystal	0.04	0.04	-	Current	Yes but colored	1
LiCl-C_3N_4	0.9	1.4	3.5	Resistive	Not mentioned	2
LiCl loaded HPPMs	2	32	4	Resistive	Not mentioned	3
Ag@mpg-CN	3	1.4	0.6	Resistive	Not mentioned	4
In–SnO_2 loaded g-C_3N_4	3.5	1.5	0.7	Resistive	Not mentioned	5
PEDOT:PSS/PUD	3.5	7	-	Resistive	Yes	6
WS_2	5	6	-	Current	Yes but colored	7
CKF	6.0	10.8	<0.57	Resistive	Yes	*This work*
CVD-graphene	6	20	-	Resistive	Not mentioned	8
MgO-KCl/SiO_2	6	26	4	Resistive	Not mentioned	9
MoS_2	9	17	-	Resistive	Not mentioned	10
MgO/SBA-15	10	20	2	Resistive	No	11
WS_2	~12	~13	-	Current	Yes but colored	12
MoS_2/GO nanocomposite	43	37	3~30	Current	Not mentioned	13
GO/PSS composite	60	50	-	Capacitive	Not mentioned	14
Li/SBA-15	60	180	3	Resistive	Not mentioned	15
Gallium-doped ZnO	70	90	4.8	Resistive	Yes but colored	16
VS_2	30~40	12~50	-	Resistive	Not mentioned	17
SnO_2/RGO hybrid nanocomposite	6~102	6~9	-	Capacitive	Not mentioned	18
SnO_2 nanowire	120~170	20~60	-	Resistive	Not mentioned	19
Graphene oxide resistive humidity sensor	189±49	89±5	5	Resistive	Not mentioned	20
V_2O_5 nanosheet	~240	~300	-	Resistive	Not mentioned	21
Perovskite $CH_3NH_3PbBr_3$	250	30~70	-	Fluorescence	Not mentioned	22
Black phosphorus	255	10	-	Resistive	Not mentioned	23

Table S2. Electrical resistance (MΩ) of CKF within 5 weeks in 11.3 % – 97.3 % RH range.

Week / % RH	0	1	2	3	4	5	Average change per week [%]
11.3	435.23	440.12	423.43	435.71	423.22	428.27	2.38
23.0	144.72	148.23	148.95	152.96	140.46	145.41	3.46
32.8	78.67	80.36	85.81	87.81	75.38	78.38	5.88
40.0	48.07	50.81	45.32	48.32	45.72	42.72	7.01
43.2	39.25	39.78	39.58	39.48	39.17	39.22	0.60
53.0	15.24	15.55	15.74	16.74	15.14	16.04	5.02
67.0	6.91	6.91	6.74	6.94	6.91	6.96	1.27
75.3	3.27	3.28	3.25	3.56	3.29	3.21	3.96
85.1	1.84	1.84	1.86	1.96	1.89	1.91	2.21
97.3	0.33	0.32	0.38	0.38	0.34	0.36	7.44

Table S3. Comparison of data measured by CKF-based skin moisture detector with that by commercial skin moisture detector, in the "sweating" experiment.

Measurement method	Parts of body	About to running	Time after running						
			0 min	1 min	2 min	3 min	4 min	5 min	6 min
CKF-based skin moisture detector	Palm	40 %	45 %	46 %	47 %	46 %	45 %	42 %	41 %
	Back	46 %	55 %	61 %	57 %	50 %	46 %	42 %	37 %
	Forehead	20%	47 %	42 %	36 %	35 %	33 %	33 %	32 %
Commercial skin moisture detector	Palm	38.51 %	45.22 %	45.95 %	47.03 %	46.41 %	45.33 %	42.14 %	40.85 %
	Back	46.34 %	55.23 %	61.65 %	57.12 %	50.18 %	46.78 %	42.47 %	37.04 %
	Forehead	20.52 %	47.15 %	42.69 %	36.82 %	34.93 %	33.67 %	33.86 %	31.05 %

Table S4. Comparison of data measured by CKF-based skin moisture detector with that measured by commercial skin moisture detector, in the "moisturizing" experiment.

Measurement method	Moisturizer	About to washing	Time after washing and wiping						
			0 min	0.5 min	1.0 min	1.5 min	2.0 min	2.5 min	3.0 min
CKF-based skin moisture detector	Without	20 %	58 %	48 %	36 %	28 %	26 %	24 %	21 %
	With	24 %	51 %	50 %	49 %	43 %	36 %	35 %	36 %
Commercial skin moisture detector	Without	20.61 %	58.30 %	48.02 %	36.62 %	28.38 %	26.07 %	24.14 %	21.17 %
	With	24.61 %	51.36 %	50.10 %	49.53 %	43.09 %	36.55 %	35.04 %	36.43 %

References

1. Kano, S.; Kim, K.; Fujii, M., Fast-response and Flexible Nanocrystal-based Humidity Sensor for Monitoring Human Respiration and Water Evaporation on Skin. *ACS sensors* **2017,** *2* (6), 828-833.
2. Zhang, Z.; Huang, J.; Yuan, Q.; Dong, B., Intercalated Graphitic Carbon Nitride: a Fascinating Two-Dimensional Nanomaterial for an Ultra-sensitive Humidity Nanosensor. *Nanoscale* **2014,** *6* (15), 9250-9256.
3. Jiang, K.; Zhao, H.; Dai, J.; Kuang, D.; Fei, T.; Zhang, T., Excellent Humidity Sensor Based on LiCl Loaded Hierarchically Porous Polymeric Microspheres. *ACS applied materials & interfaces* **2016,** *8* (38), 25529-25534.
4. Tomer, V. K.; Thangaraj, N.; Gahlot, S.; Kailasam, K., Cubic Mesoporous Ag@ CN: a High Performance Humidity Sensor. *Nanoscale* **2016,** *8* (47), 19794-19803.
5. Malik, R.; Tomer, V. K.; Chaudhary, V.; Dahiya, M. S.; Sharma, A.; Nehra, S.; Duhan, S.; Kailasam, K., An Excellent Humidity Sensor Based on In–SnO 2 Loaded Mesoporous Graphitic Carbon Nitride. *Journal of Materials Chemistry A* **2017,** *5* (27), 14134-14143.
6. Trung, T. Q.; Ramasundaram, S.; Lee, N.-E., Transparent, Stretchable, and Rapid-response Humidity Sensor for Body-attachable Wearable Electronics. *Nano Research* **2017,** *10* (6), 2021-2033.
7. Guo, H.; Lan, C.; Zhou, Z.; Sun, P.; Wei, D.; Li, C., Transparent, Flexible, and Stretchable WS2 Based Humidity Sensors for Electronic Skin. *Nanoscale* **2017,** *9* (19), 6246-6253.
8. Smith, A. D.; Elgammal, K.; Niklaus, F.; Delin, A.; Fischer, A. C.; Vaziri, S.; Forsberg, F.; Råsander, M.; Hugosson, H.; Bergqvist, L., Resistive Graphene Humidity Sensors with Rapid and Direct Electrical Readout. *Nanoscale* **2015,** *7* (45), 19099-19109.
9. Geng, W.; Yuan, Q.; Jiang, X.; Tu, J.; Duan, L.; Gu, J.; Zhang, Q., Humidity Sensing Mechanism of Mesoporous MgO/KCl–SiO2 Composites Analyzed by Complex Impedance Spectra and Bode Diagrams. *Sensors and Actuators B: Chemical* **2012,** *174*, 513-520.
10. Zhang, S.-L.; Choi, H.-H.; Yue, H.-Y.; Yang, W.-C., Controlled Exfoliation of Molybdenum Disulfide for Developing Thin Film Humidity Sensor. *Current Applied Physics* **2014,** *14* (3), 264-268.
11. Wang, R.; Liu, X.; He, Y.; Yuan, Q.; Li, X.; Lu, G.; Zhang, T., The Humidity-sensitive Property of MgO-SBA-15 Composites in One-pot Synthesis. *Sensors and Actuators B: Chemical* **2010,** *145* (1), 386-393.
12. Pawbake, A. S.; Waykar, R. G.; Late, D. J.; Jadkar, S. R., Highly Transparent Wafer-scale Synthesis of Crystalline WS2 Nanoparticle Thin Film for Photodetector and Humidity-sensing Applications. *ACS applied materials & interfaces* **2016,** *8* (5), 3359-3365.
13. Burman, D.; Ghosh, R.; Santra, S.; Guha, P. K., Highly Proton Conducting MoS2/Graphene Oxide Nanocomposite Based Chemoresistive Humidity Sensor. *Rsc Advances* **2016,** *6* (62), 57424-57433.
14. Yu, H.-W.; Kim, H. K.; Kim, T.; Bae, K. M.; Seo, S. M.; Kim, J.-M.; Kang, T. J.; Kim, Y. H., Self-powered Humidity Sensor Based on Graphene Oxide Composite Film Intercalated by Poly (Sodium 4-styrenesulfonate). *ACS applied materials & interfaces* **2014,** *6* (11), 8320-8326.

15. Zhang, T.; Wang, R.; Geng, W.; Li, X.; Qi, Q.; He, Y.; Wang, S., Study on Humidity Sensing Properties Based on Composite Materials of Li-doped Mesoporous Silica A-SBA-15. *Sensors and Actuators B: Chemical* **2008,** *128* (2), 482-487.

16. Su, P.-G.; Tseng, J.-Y.; Huang, Y.-C.; Pan, H.-H.; Li, P.-C., Novel Fully Transparent and Flexible Humidity Sensor. *Sensors and Actuators B: Chemical* **2009,** *137* (2), 496-500.

17. Feng, J.; Peng, L.; Wu, C.; Sun, X.; Hu, S.; Lin, C.; Dai, J.; Yang, J.; Xie, Y., Giant Moisture Responsiveness of VS2 Ultrathin Nanosheets for Novel Touchless Positioning Interface. *Advanced materials* **2012,** *24* (15), 1969-1974.

18. Zhang, D.; Chang, H.; Li, P.; Liu, R.; Xue, Q., Fabrication and Characterization of an Ultrasensitive Humidity Sensor Based on Metal Oxide/graphene Hybrid Nanocomposite. *Sensors and Actuators B: Chemical* **2016,** *225*, 233-240.

19. Kuang, Q.; Lao, C.; Wang, Z. L.; Xie, Z.; Zheng, L., High-sensitivity Humidity Sensor Based on a Single SnO2 Nanowire. *Journal of the American Chemical Society* **2007,** *129* (19), 6070-6071.

20. De Luca, A.; Santra, S.; Ghosh, R.; Ali, S.; Gardner, J.; Guha, P.; Udrea, F., Temperature-modulated Graphene Oxide Resistive Humidity Sensor for Indoor Air Quality Monitoring. *Nanoscale* **2016,** *8* (8), 4565-4572.

21. Pawar, M. S.; Bankar, P. K.; More, M. A.; Late, D. J., Ultra-thin V2O5 Nanosheet Based Humidity Sensor, Photodetector and its Enhanced Field Emission Properties. *RSC Advances* **2015,** *5* (108), 88796-88804.

22. Xu, W.; Li, F.; Cai, Z.; Wang, Y.; Luo, F.; Chen, X., An Ultrasensitive and Reversible Fluorescence Sensor of Humidity Using Perovskite CH3NH3PbBr3. *Journal of Materials Chemistry C* **2016,** *4* (41), 9651-9655.

23. Late, D. J., Liquid Exfoliation of Black Phosphorus Nanosheets and its Application as Humidity Sensor. *Microporous and Mesoporous Materials* **2016,** *225*, 494-503.